https://doi.org/10.3311/PPme.42722
Creative Commons Attribution

Periodica Polytechnica Mechanical Engineering, 70(1), pp. 51–58, 2026

Reconstruction of 3D Floating Body Motion on Shallow Water Flows Using the Smoothed Particle Hydrodynamics Method

Balázs Havasi-Tóth[1,2], Balázs Farkas[1*]

[1] Department of Fluid Mechanics, Faculty of Mechanical Engineering, Budapest University of Technology and Economics, Műegyetem rkp. 3., H-1111 Budapest, Hungary
[2] HUN-REN-BME Morphodynamics Research Group, Budapest University of Technology and Economics, Műegyetem rkp. 3., H-1111 Budapest, Hungary
[*] Corresponding author, e-mail: farkas.balazs@gpk.bme.hu

Received: 04 November 2025, Accepted: 07 January 2026, Published online: 12 January 2026

Abstract

The investigation of floating body motions is a frequently visited topic in the areas of wave energy converters and coastal engineering. In fluvial conditions, the design process of floating platforms and the forecast of ice jamming events are also parts of relevant applications. Apparently, the two-way coupling of the fluid and floating body forces is often a fundamental requirement in such applications leading to computationally expensive studies. In cases of open surface flow modeling, where the water depth is sufficiently small compared to the horizontal extensions of a water body, the depth-averaged shallow water equations (SWE) offer an efficient alternative of the 3D Navier-Stokes equations. Utilizing the benefits of the SWEs, we aim to reduce the 3D problem of floating body motions to the 2D shallow water framework utilizing the smoothed particle hydrodynamic (SPH) method. However, the task is not straightforward due to the explicit nature of the SWE-SPH model. As an additional constraint, the presence of a floating object determines the local water depth, which is otherwise purely driven by the equation of motion and continuity. In our model, this constraint is defined by an additional penalty term in the equation of motion to accurately predict the water depth as well as the forces acting on the floating object. As a result, a two-way coupled fluid structure interaction model is established. The proposed method is easy to be implemented and offers an efficient alternative approach to the fully resolved computations, with a reasonable loss of accuracy.

Keywords

smoothed particle hydrodynamics, shallow water equation, floating body, wave response

1 Introduction

Smoothed Particle Hydrodynamics (SPH) is a highly efficient tool in modeling violent free surface flows due to the automatic reproduction of the surface elevation and exact conservation of mass. Since its initial appearance in 1977 by Lucy [1] and independently by Gingold and Monaghan [2], SPH went through significant developments in countless areas of scientific and engineering applications. Opening new perspectives, the first applications of SPH in modeling free surface coastal flows were published in the 1990's by Monaghan [3], and Monaghan and Kos [4]. At the end of the same decade, Wang and Shen [5] proposed the first implementation of the SPH method on reduced dimensionality in terms of the water depth. Ata and Soulaïmani [6] improved the stability of the model by means of a dissipation term based on a Riemann solver. A corrected variational formulation of the SPH method for shallow water equations was proposed by Rodriguez-Paz and Bonet [7]. Further improvements on the SWE-SPH (Shallow Water Equation with Smoothed Particle Hydrodynamics) model were presented by De Leffe et al. [8] in terms of more uniform particle distributions, and the balancing of the source terms in the case of discontinuous bed elevations by Vacondio et al. [9] and Xia et al. [10]. More recently, the SWE-SPH model has been successfully applied for tsunami and debris flow modeling by Omidvar et al. [11], Pastor et al. [12], Pastor et al. [13] and Aslami et al. [14]. A two-way coupling technique mutually providing proper boundary conditions to adjacent domains governed by the Navier-Stokes and shallow water equations through SPH is presented by Ni et al. [15].

Cite this article as: Havasi-Tóth, B., Farkas, B. "Reconstruction of 3D Floating Body Motion on Shallow Water Flows Using the Smoothed Particle Hydrodynamics Method", Periodica Polytechnica Mechanical Engineering, 70(1), pp. 51–58, 2026. https://doi.org/10.3311/PPme.42722

Fluid structure interactions (FSI), and the dynamics of floating bodies in particular, attract increasing attention in the field of coastal engineering. The reason is that the necessity of the utilization of renewable energy sources became exceptionally pressing. Furthermore, other applications, such as the design processes of coastal or fluvial floating structures or the forecast of ice jamming on rivers and in coastal environment also show interest in the topic. Consequently, the investigation of floating body motions became a frequently referred topic in case of the SPH method as well. The earliest successful attempts on modeling simple floating object excited by surface waves were published by Doring et al. [16], Manenti et al. [17] and Rogers et al. [18]. Yeylaghi et al. [19] discussed the motion of a point absorber over offshore waves. Ren et al. [20] and Domínguez et al. [21] showed that the motion of floating structures with moorings in coastal shallow water environment reproduces experimental data with a remarkable accuracy. A detailed review of the recent developments in ocean energy devices is presented by Lyu et al. [22].

The relevance of the topic recently motivated the development of SPH solvers to construct multiphysics tools. Two examples of these developments were shown by Domínguez et al. [23] and Amicarelli et al. [24].

In contrast with the aforementioned interest shown in 3D FSI applications, the same phenomena are almost completely unvisited in terms of the depth integrated shallow water SPH framework. However, the mathematical investigation of the topic is under discussion for decades. At the turn of the millennium Abul-Azm [25] proposed different approaches to the problem under shallow water conditions and oblique waves. Later, Sturova [26] implied the effects of uneven topography, while Meylan and Sturova [27] extended the investigation with elastic structures. More recently, the effects of shallow water on wave energy converters were visited by Sinha et al. [28].

The aim of our work is to construct a simple yet effective model on the problem of floating body motions subject to 2D shallow water conditions. We applied the SWE-SPH model as proposed by Xia et al. [10] and employ an additional term in the momentum equation to form a two-way coupled model of floating objects on shallow water. For the construction of the simulations in this paper, we used the open-source general-purpose particle-based computational tool Nauticle introduced by Havasi-Tóth [29].

2 The SWE–SPH model

In the present work we adopted the well-balanced SPH shallow water model proposed by Xia et al. [10]. Here we briefly present the model without the detailed deduction. In the present work the governing equations are interpreted in the Lagrangian frame of reference, using the total time derivative as $d\circ/dt = \partial\circ/\partial t + \boldsymbol{v}\nabla\circ$. Here $\boldsymbol{v} = v(\boldsymbol{r}, t)$ is the velocity field and $\boldsymbol{r}$ is the spatial coordinate, respectively.

The continuity and momentum equations governing depth integrated shallow water flows can be written as:

$$\frac{db}{dt} = -b\nabla\boldsymbol{v}, \quad \frac{d\boldsymbol{v}}{dt} = -g\left(\nabla b + \nabla z\right) - g\frac{n^2\boldsymbol{v}\boldsymbol{v}}{b^{4/3}}, \tag{1}$$

where $b = b(\boldsymbol{r}, t)$, $z = z(\boldsymbol{r})$, n, g and $\boldsymbol{r}$ are the water depth, bed elevation, Manning's roughness coefficient and the magnitude of the gravitational acceleration. For later reference, we recall the mathematical analogy between the shallow-water equations (Eq. (1)) and the governing equations of two-dimensional compressible gas flow in dimensionless form, where the water depth corresponds to the gas density [30].

Following the deduction introduced by Xia et al. [10], the SPH-discretized discretized form of Eq. (2) then reads as:

$$\begin{aligned} b_i &= \sum_j^N V_j W_{ij} - \sum_j^N \frac{V_j}{b_j}\left(z_i - z_j\right)W_{ij}, \\ \frac{d\boldsymbol{v}}{dt} &= -\sum_j^N\left(gV_j + \frac{V_j}{b_j}\Pi_{ij}\right)\nabla W_{ij} \\ &-g\sum_j^N\frac{V_j}{b_j}\left(z_j - z_i\right)\nabla W_{ij} - g\frac{n^2\boldsymbol{v}_i\boldsymbol{v}_i}{b^{4/3}}, \end{aligned} \tag{2}$$

where $W_{ij} = W^q\left(\left\|\boldsymbol{r}_i - \boldsymbol{r}_j\right\|, h\right)$ is the fifth order polynomial smoothing kernel function:

$$W_{ij} = \frac{7}{4\pi h^2}\left(1 - \frac{\boldsymbol{r}_i - \boldsymbol{r}_j}{2h}\right)\left(1 + 2\frac{\boldsymbol{r}_i - \boldsymbol{r}_j}{h}\right), \tag{3}$$

constructed by Wendland [31], V_j is the volume associated to particle j, h is the smoothing radius and Π_{ij} denotes the artificial viscosity term (mutatis mutandis) proposed by Morris et al. [32]. Note that the depth variable b in the discretized continuity equation appears on both sides of equation. Instead of the application of a high complexity implicit method, Xia et al. [10] proposed a simple workaround through an iterative approach. Accordingly, the consecutive evaluation of the depth formula with an initial guess of:

$$b_i^0 = \sum_j^N V_j W_{ij}, \tag{4}$$

is performed when the bed elevation is not globally constant. As they pointed out, a few steps of the iteration provide appropriate accuracy in terms of the water depth. Nevertheless, it can be seen that the explicit definition of

the water depth cannot be done without making additional considerations and computational steps.

In order to maintain the proper particle sampling in the case of spatially changing water depth, a variable smoothing radius is applied as:

$$h_i = h_0 \left(\frac{b_0}{b_i} \right)^{\frac{1}{d}}, \tag{5}$$

where d is the problem dimension, while h_0 and b_0 are the initial smoothing radius and water depth respectively. In this paper, we investigate two-dimensional cases, therefore we set $d = 2$.

2.1 Water depth constraint by a penalty term

We consider a shallow water body with a large structure floating on the surface with a draft less than $b/2$. The limitation is made here to avoid the rapid deterioration of numerical accuracy and convergence in regions of very low water depths, where h would grow unreasonably high due to Eq. (5). In the prescribed case, the depth of the water – which is otherwise driven by Eq. (2) – at that location is constrained by the elevation (i.e., draft) of the structure. As was mentioned earlier, in analogy with the density in terms of the weakly compressible variant of SPH, there is no obvious and explicit way to prescribe the water depth in Eq. (2). Therefore, an additional penalty term is proposed in the momentum equation to set the required depth b at the given locations [33].

The idea of enforcing a locally desired depth constraint b_d is the introduction of a source term in the momentum equation as:

$$\frac{d\boldsymbol{v}}{dt} = -g\left(\nabla b + \nabla z + \nabla b^*\right) - g\frac{n^2 \boldsymbol{v}\boldsymbol{v}}{b^{4/3}}, \tag{6}$$

in which the function $b^* = b^*(\varepsilon)$ is computed using the depth error function:

$$\varepsilon(\boldsymbol{r},t) = b(\boldsymbol{r},t) - b_d(\boldsymbol{r},t), \tag{7}$$

where b_d is the desired depth under the floating object. Motivated by the proportional-integral-derivative (PID) control theory, we propose the application of a PID control function [34] to reduce the residual error. Applied to the error function ε, this yields:

$$b^*(\boldsymbol{r},t) = K_P \varepsilon(\boldsymbol{r},t) + K_I \int_0^T \varepsilon(\boldsymbol{r},t)\,dt + K_D \frac{d\varepsilon(\boldsymbol{r},t)}{dt}, \tag{8}$$

where K_P, K_I and K_D are the corresponding proportional integral and derivative gains. In the subsequent paragraphs, we introduce the application of Eq. (8) in the SWE-SPH method considering that the desired depth function b_d is deduced from a spatially fixed or freely moving solid floating structure on the water surface.

Firstly, we define two layers of particles in the domain to specify the overlapping fluid and solid regions.

The fluid particles lay in the xy plane according to Fig. 1. Solid particles, forming the rigid body, are capable of moving in three dimensions, however, their planar projected location is used in Eq. (6) during the computation and their vertical position is assigned to them as a field variable a (cf. Fig. 1). The determination of the interaction between the solid and fluid particles and the computation of Eq. (7) is explained in the followings. In order for an improved prescription of the structure geometry, the interparticle distances are determined according to:

$$dx_f = 2dx_s, \tag{9}$$

where the subscripts f and s mark the fluid and solid particles. Hereinafter, the volume ratio is considered to be $V_f = 4V_s$ as a consequence of Eq. (9). The two layers of particles are distinguished by the color function C_0, as $C_0 = 0$ for the fluid, and $C_0 = 1$ for the solid particles. Considering a unit water depth b_j for the sampling operator, we then sample the C field at the fluid particles as:

$$C_i = \sum_j^N C_0 V_j W_{ij}, \tag{10}$$

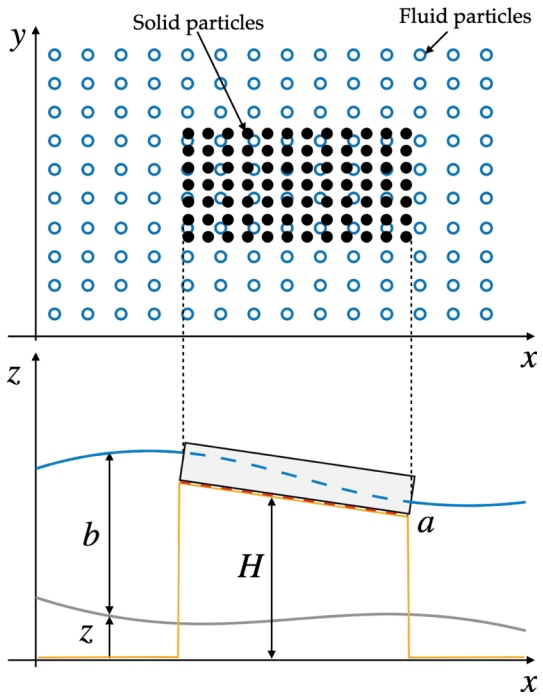

Fig. 1 The 2D dual layer of particles (top) and the schematic explanation of the model (bottom) with the functions required by the penalty term

to mark the fluid particles that are in interaction with the structure. Using the computed C field, the desired water surface elevation H under the structure is approximated using the abovementioned structure elevation as:

$$H_i = \sum_j^N a_j V_j C_j W_{ij}. \tag{11}$$

The real water surface elevation at a fluid particle i, which is by definition:

$$S_i = b_i + z_i, \tag{12}$$

Is applied when computing the error function of the depth as:

$$\varepsilon_i = S_i C_i - H_i, \tag{13}$$

which is in agreement with Eq. (7) in the discretized system. Then, the penalty term – controlling the depth – is constructed according to the error function of both the proportional and integral terms as:

$$\begin{aligned} b_i^* &= K_P \varepsilon_i + K_I \int_0^t \varepsilon_i dt + K_D \frac{d\varepsilon_i}{dt} \\ &\approx K_P \varepsilon_i + K_I \sum_{k=0}^{k_c} \Delta t^k \varepsilon_i^k + K_D \frac{\varepsilon_i^k - \varepsilon_i^{k-1}}{\Delta t}, \end{aligned} \tag{14}$$

where again, the K_P, K_I and K_D are the gain values of the proportional, integral and derivative terms respectively, k is the index of time levels in the simulation and k_c is the current time level. Note, that the integration term is employed to completely eliminate the "imaginary" vertical overlap between the fluid surface and the solid body without using an infeasibly high stiffness parameter K_P.

We found that the gains $K_P = 4$, $K_I = 4\sqrt{g/b_0}$ and $K_I = 4\sqrt{b_0/g}$ provide sufficiently low residual error values in the investigated cases and applied them throughout the rest of the paper.

Finally, the equation of motion can be completed with the additional term to obtain:

$$\begin{aligned} \frac{d\boldsymbol{v}}{dt} &= -\sum_j^N \left(gV_j + \frac{V_j}{b_j} \Pi_{ij} \right) \nabla W_{ij} \\ &- g \sum_j^N \frac{V_j}{b_j} \left(z_j - z_i \right) \nabla W_{ij} \\ &- g b_i \sum_j^N \left(\frac{b_i^*}{b_i^2} + \frac{b_j^*}{b_j^2} \right) V_j \nabla W_{ij} - g \frac{n^2 \boldsymbol{v}_i}{\boldsymbol{v}_i} \sigma_i, \\ \sigma_i &= C_i \left[\left(1 - \frac{1}{C_i} \right) \frac{n^2 \boldsymbol{v}_i}{b_i^{4/3}} - \left(\frac{2^{0.63} \boldsymbol{v}_i}{8.5 b_i^{0.63}} \right)^{\frac{1}{0.54}} \right], \end{aligned} \tag{15}$$

where σ collects the Manning and Hazen-Williams [35] hydraulic losses with respect to the flows with free surface as well as the areas closed by the structure. It is worth mentioning that the fictitious water surface level that would be locally present in the lack of solid structure can be produced by:

$$b_i^f = b_i + \varepsilon_i, \tag{16}$$

but further investigation of this field is out of scope of the present work.

The equations presented above (Eqs. (10)–(15)) for all fluid particles are evaluated at each time step. As a coupling function between the solid and fluid domains, the b^* field can also be utilized during the computation of the force distribution acting on the solid structure. Besides the gravitational acceleration – following Newton's third law – b^* is therefore accountable for the time and space dependent load of the floating structure. In simple words, b^* determines the vertical hydraulic load, which is expected to be in equilibrium with the weight of the structure in a hydrostatic problem.

Nevertheless, in case of a hydrodynamic problem, b^* is still applicable to compute the dynamic loads, but another set of equations for the structure should be defined. In 3D, Newton's second law infers that the motion of the involved rigid body constructed by particles are governed by the equations expressed as:

$$\begin{aligned} M\dot{\boldsymbol{u}} &= -\left(\boldsymbol{g}M + \boldsymbol{F}_j \right) \boldsymbol{e}_z, \\ \boldsymbol{\Theta}\dot{\boldsymbol{\omega}} &= \sum_j^N \left(\boldsymbol{r}_{cg} - \boldsymbol{r}_j \right) \times \left(\boldsymbol{F}_j \boldsymbol{e}_z \right) + \boldsymbol{\omega} \times \boldsymbol{\pi}_{rg}, \\ \boldsymbol{F}_j &= \sum_j^N \rho_w \boldsymbol{g} \left(1 - C_{oj} \right) \frac{V_j}{b_j} b^*, \end{aligned} \tag{17}$$

where M, $\boldsymbol{u}$, $\boldsymbol{\Theta}$, $\boldsymbol{\omega}$ and $\boldsymbol{r}_{cg}$ are the mass, velocity, mass moment of inertia, angular velocity and position of the center of gravity of the rigid body. The angular momentum with respect to $\boldsymbol{r}_{cg}$ is denoted by $\boldsymbol{\pi}_{rg}$. Note that the factor $(1 - C_{oj})$ in the force calculation is required because the sampling must occur on the solid body particles but only the fluid particles should be taken into account. By means of Eq. (17), the 3D motion of the structure is computed, and the corresponding particle positions are projected on the xy plane to perform the samplings properly. Since the angles of the structure remain small in case of reasonable wave amplitudes, we do not consider the deviations of the projected interparticle distances from the original layout during the solution process. In the present work, we performed the computations using a velocity Verlet integration scheme and applied the same time

step size in both systems of ordinary differential equations (ODE) in Eqs. (15) and (17).

The relevance of the proposed model is that the three-dimensional motion of a floating structure can be reconstructed using the significantly less expensive shallow water equations.

3 Results

3.1 Test I.: stationary platform

The first test case we introduce implies a 90 × 30 m rectangular and flat floating pontoon over a shallow river with an average velocity of ~3 m/s. In this case, the structure is fixed in space in both the vertical and horizontal directions. For the sake of simplicity, the bed topography is given by the piecewise linear-constant function:

$$z(y)=\begin{cases}0.05y-5.5, & \text{if } y\geq 50,\\ -3 & \text{otherwise,}\end{cases}$$

where y is the spanwise direction. Thus the bed gradient can be determined analytically at any location in the domain. The schematic layout is presented in Fig. 2, with the preset structure elevation of 0.8 m. The applied boundary conditions were periodic in the x-direction with a channel length of 300 m and symmetric in the y-direction. Since the bed elevation was set to constant in streamwise direction, the moment source was implemented through a hydraulic gradient of 0.05, which results in a river flow with a relatively strong current. The applied average interparticle distance was set to dx_f = 1.22 m. Manning's parameter, controlling the hydraulic losses was chosen to be n = 0.05 s/m$^{1/3}$.

As it is shown in Fig. 3, the structure significantly affects the free surface shape, which has a peak of 0.93 m at the front stagnation point of the structure, while the surface height at rest would be 0.1 m. Since the floating structure induces an increased surface elevation at the leading edge as expected, spanwise components of the velocity vectors appear below the structure due to the larger head between the shore and the structure. Furthermore, a convective

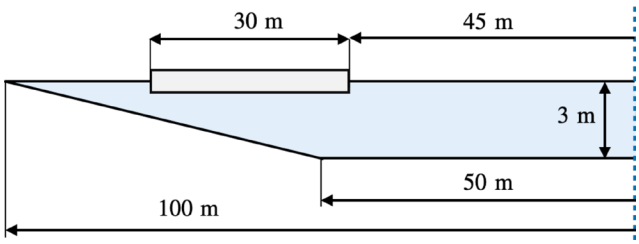

Fig. 2 The schematic layout of the first test case with spatially fixed solid structure. The vertical dashed line marks the symmetric boundary condition. Schematic not to scale

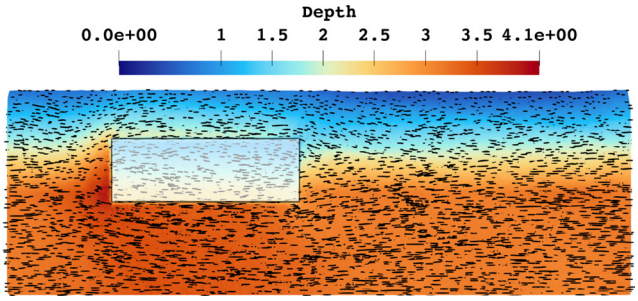

Fig. 3 Free surface elevation in the case of the fixed structure on the shallow water flow with a Delaunay-triangulation of the fluid particles. Note that the solid body particles are hidden due to better visualization

acceleration at the front region below the leading edge is formed due to the suddenly narrowed cross section area showing a qualitative match with the expectations.

3.2 Test II.: wave response of a floating structure

In our second test case, we present the wave response of a flat floating structure in a wave tank of length L = 13.024 m. The applied wave generation and dissipation approach follows the method presented by Schmitt et al. [36] as:

$$\begin{aligned}a_w &= 2\sin\left(f_w 2\pi t\right),\\ a_b &= 6\left(-2X^3+3X^2\right)\boldsymbol{v},\\ X &= \frac{L_{bch}+\left(x+\frac{L}{2}\right)-L}{L_{bch}},\end{aligned} \tag{18}$$

where a_w and a_b are the wave generator and absorption terms respectively added to the system Eq. (15) in the x-direction, f_w = 0.7 Hz is the excitation frequency and L_{bch} = 2.96 m is the length of the wave absorber regions at both ends of the tank. In accordance with the 0.02 m initial draft of the structure of 1.0 × 0.8 m base size, its mass is 17.42 kg, while the water depth at rest is b_0 = 0.2 m.

The schematic layout of the problem is shown in Fig. 4. Each of the mooring cables at the corners of the structure are implemented as sequentially coupled 16 linear springs

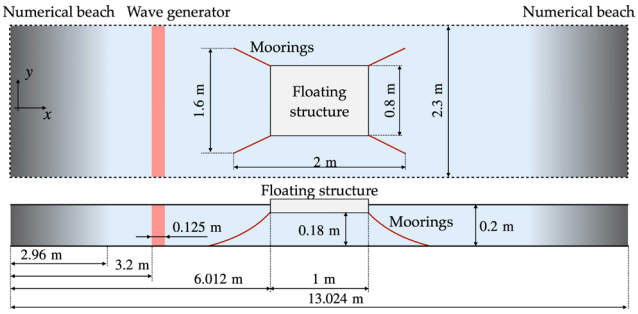

Fig. 4 Initial layout of the wave tank with the wave generator and wave absorbers and the moored floating structure in the center. Schematic not to scale

with a strength of s = 20 N/m and a damping coefficient of k = 0.01 Ns/m. The mass of each cable was m_p = 0.008 kg uniformly distributed over the spring joints and the total length of the cables were 0.581 m. Similarly to the rigid body model, the moorings were also considered three-dimensional, but no interactions with the water were taken into account. The resulting system therefore a four-way weakly coupled model as presented in Fig. 5. As was already mentioned, the springs along the mooring cables are connected through joints. The instantaneous force of each spring is defined according to:

$$\boldsymbol{F}_s = -k\frac{\boldsymbol{r}_{R,L}}{\boldsymbol{r}_{R,L}^2}\left(\boldsymbol{v}_{R,L}\boldsymbol{r}_{R,L}\right) - s\frac{\boldsymbol{r}_{R,L}}{\boldsymbol{r}_{R,L}}\left(\boldsymbol{r}_{R,L} - d_0\right), \tag{19}$$

where $\boldsymbol{r}_{R,L}$ is the vector between the right and left joints of the spring, $\boldsymbol{v}_{R,L}$ is the relative velocity of the two joints and d_0 = 0.0363 m is the initial length of the cable segments. For the sake of simplicity, we applied symmetric boundary conditions on all four sides of the channel. Besides the application of the ratio in Eq. (9), the particle resolution of the water body in the present case was dx_f = w/78, where w = 2.3 m is the width of the wave tank.

To validate our results, the problem was reconstructed in ANSYS AQWA [37]. ANSYS AQWA applies potential flow theory to solve the linearized boundary-value problem for inviscid, incompressible, and irrotational fluid motion, using boundary element (panel) methods to model wave–body interactions, and is broadly recognized in both industry and research as a reliable method for analyzing wave-structure interaction and floating-body responses [38].

The estimated values of the response amplitude operator (RAO) are defined as the ratio of the structure's oscillation amplitudes and the wave excitation amplitudes at different excitation frequencies are presented in Fig. 6. The sources of the errors between the two models may originate from the comparison of two models with inherently different methodology and the additional dynamics introduced by the penalty term in the SPH method.

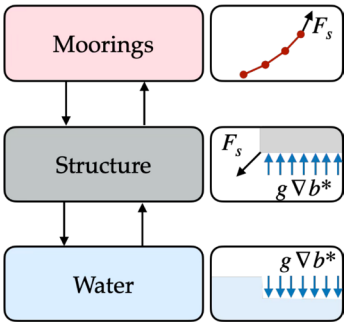

Fig. 5 Schematic of the coupling applied in Test II. Double arrays indicate two-way couplings between the different components

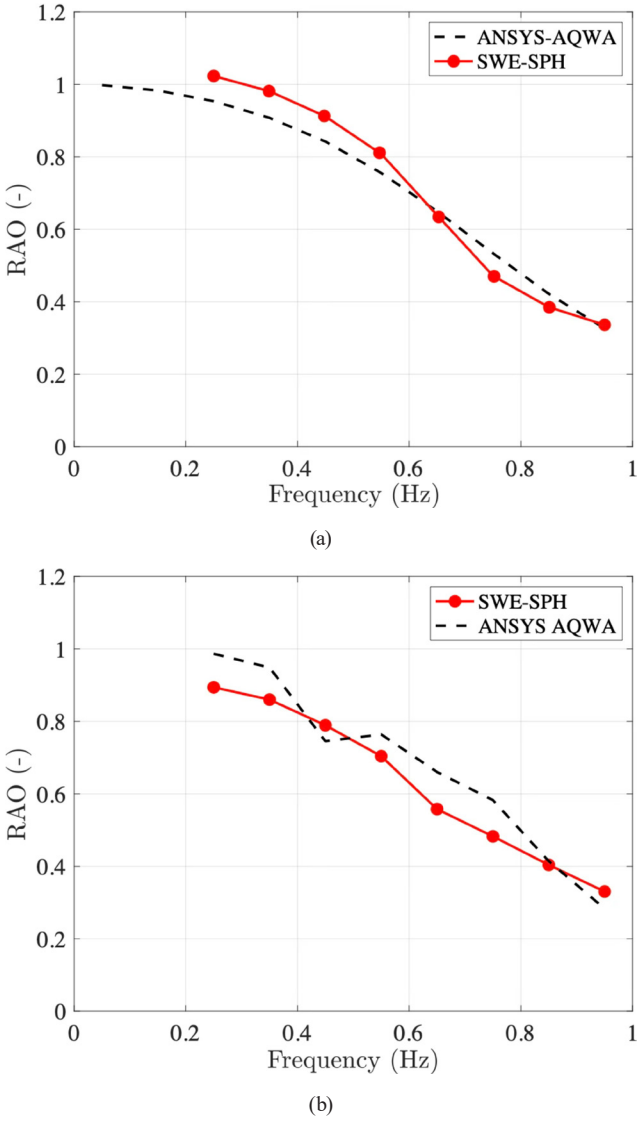

Fig. 6 Response amplitude operator (RAO) of the structure as a function of the excitation frequencies: (a) Free object; (b) Object with mooring cables

Although further improvements of the model would be possible, experimental investigations would be required for tuning the control parameters more accurately. Based on the presented results the SPH-SWE model is capable of capturing the model's motion under various wave conditions with sufficient accuracy.

4 Conclusions

In this paper we propose a modification of the shallow water momentum equation to become applicable for the investigation of the three-dimensional motion of structures floating on shallow water bodies. We introduced the idea of an additional source term assuring the water surface to obey the geometric constraint determined by the floating structure. In order for a feasible model to be built, besides a proportional gain, we employed an integral

gain in the penalty term, by which the residual error of the surface elevation is significantly reduced. The floating structure can either be fixed in space or governed by the three-dimensional rigid body dynamics.

Both configurations are tested through the test cases:

- Test I: a fixed floating pontoon is investigated in a river flow with relatively high velocities,
- Test II: a floating rigid body motion with mooring cables is reproduced in a numerical wave tank.

The subject of our focus leads to interesting analogy with the weakly compressible variant of SPH, where the penalty term might be employed as a constraint on the density field. This would potentially lead to slightly better performance in terms of eliminating undesired residual deviations of the density from the reference value. Additionally, the implementation of a derivative gain raises the idea of an artificial bulk viscosity operating in the pressure gradient term of the momentum equation.

Acknowledgement

Project no. TKP-6-6/PALY-2021 has been implemented with the support provided by the Ministry of Culture and Innovation of Hungary from the National Research, Development and Innovation Fund, financed under the TKP2021-NVA funding scheme.

References

[1] Lucy, L. B. "A numerical approach to the testing of the fission hypothesis", Astronomical Journal, 82, pp. 1013–1024, 1997. https://doi.org/10.1086/112164

[2] Gingold, R. A., Monaghan, J. J. "Smoothed particle hydrodynamics: theory and application to non-spherical stars", Monthly Notices of the Royal Astronomical Society, 181(3), pp. 375–389, 1977. https://doi.org/10.1093/mnras/181.3.375

[3] Monaghan, J. J. "Simulating Free Surface Flows with SPH", Journal of Computational Physics, 110(2), pp. 399–406, 1994. https://doi.org/10.1006/jcph.1994.1034

[4] Monaghan, J. J., Kos, A. "Solitary Waves on a Cretan Beach", Journal of Waterway, Port, Coastal, and Ocean Engineering, 125(3), pp. 145–155, 1999. https://doi.org/10.1061/(ASCE)0733-950X(1999)125:3(145)

[5] Wang, Z., Shen, H. T. "Lagrangian Simulation of One-Dimensional Dam-Break Flow", Journal of Hydraulic Engineering, 125(11), pp. 1217–1220, 1999. https://doi.org/10.1061/(ASCE)0733-9429(1999)125:11(1217)

[6] Ata, R., Soulaïmani, A. "A stabilized SPH method for inviscid shallow water flows", International Journal for Numerical Methods in Fluids, 47(2), pp. 139–159, 2005. https://doi.org/10.1002/fld.801

[7] Rodriguez-Paz, M., Bonet, J. "A corrected smooth particle hydrodynamics formulation of the shallow-water equations", Computers & Structures, 83(17–18), pp. 1396–1410, 2005. https://doi.org/10.1016/j.compstruc.2004.11.025

[8] De Leffe, M., Le Touzé, D., Alessandrini, B. "SPH modeling of shallow-water coastal flows", Journal of Hydraulic Research, 48(sup1), pp. 118–125, 2010. https://doi.org/10.1080/00221686.2010.9641252

[9] Vacondio, R., Rogers, B. D., Stansby, P. K., Mignosa, P. "A correction for balancing discontinuous bed slopes in two-dimensional smoothed particle hydrodynamics shallow water modeling", International Journal for Numerical Methods in Fluids, 71(7), pp. 850–872, 2013. https://doi.org/10.1002/fld.3687

[10] Xia, X., Liang, Q., Pastor, M., Zou, W., Zhuang, Y.-F. "Balancing the source terms in a SPH model for solving the shallow water equations", Advances in Water Resources, 59, pp. 25–38, 2013. https://doi.org/10.1016/j.advwatres.2013.05.004

[11] Omidvar, P., Stansby, P. K., Rogers, B. D. "SPH for 3D floating bodies using variable mass particle distribution", International Journal for Numerical Methods in Fluids, 72(4), pp. 427–452, 2013. https://doi.org/10.1002/fld.3749

[12] Pastor, M., Blanc, T., Haddad, B., Drempetic, V., Morles, M. S., Dutto, P., Stickle, M. M., Mira, P., Merodo, J. A. F. "Depth Averaged Models for Fast Landslide Propagation: Mathematical, Rheological and Numerical Aspects", Archives of Computational Methods in Engineering, 22(1), pp. 67–104, 2015. https://doi.org/10.1007/s11831-014-9110-3

[13] Pastor, M., Tayyebi, S. M., Stickle, M. M., Yagüe, Á., Molinos, M., Navas, P., Manzanal, D. "A depth integrated, coupled, two-phase model for debris flow propagation", Acta Geotechnica, 16(8), pp. 2409–2433, 2021. https://doi.org/10.1007/s11440-020-01114-4

[14] Aslami, M. H., Rogers, B. D., Stansby, P. K., Bottacin-Busolin, A. "Simulation of floating debris in SPH shallow water flow model with tsunami application", Advances in Water Resources, 171, 104363, 2023. https://doi.org/10.1016/j.advwatres.2022.104363

[15] Ni, X., Feng, W., Huang, S., Zhao, X., Li, X. "Hybrid SW-NS SPH models using open boundary conditions for simulation of free-surface flows", Ocean Engineering, 196, 106845, 2020. https://doi.org/10.1016/j.oceaneng.2019.106845

[16] Doring, M., Oger, G., Alessandrini, B., Ferrant, P. "SPH Simulations of Floating Bodies in Waves", In: Proceedings of the ASME 2004 23rd International Conference on Offshore Mechanics and Arctic Engineering, Vancouver, Canada, 2004, pp. 741–747. ISBN 0-7918-3743-2 https://doi.org/10.1115/OMAE2004-51419

[17] Manenti, S., Panizzo, A., Ruol, P., Martinelli, L. "SPH simulation of a floating body forced by regular waves", In: 3rd ERCOFTAC SPHERIC workshop on SPH applications, Lausanne, Switzerland, 2008, pp. 38–41. [online] Available at: https://www.researchgate.net/publication/266037079_SPH_simulation_of_a_floating_body_forced_by_regular_waves [Accessed: 11 November 2025]

[18] Rogers, B. D., Dalrymple, R. A., Stansby, P. K. "SPH modeling of floating bodies in the surf zone", In: Proceedings of the 31st International Conference , Hamburg, Germany, 2009, pp. 204–215. ISBN 978-981-4277-36-5
https://doi.org/10.1142/9789814277426_0017

[19] Yeylaghi, S., Moa, B., Beatty, S., Buckham, B. Oshkai, P., Crawford, C. "SPH Modeling of Hydrodynamic Loads on a Point Absorber Wave Energy Converter Hull", In: Proceedings of the 11th European Wave and Tidal Energy Conference, Nantes, France, 2015, pp. 10A1-4-1–10A1-4-7. ISBN 978-1-31564785-2 [online] Available at: https://www.researchgate.net/publication/282648734_SPH_Modeling_of_Hydrodynamic_Loads_on_a_Point_Absorber_Wave_Energy_Converter_Hull [Accessed: 11 November 2025]

[20] Ren, B., He, M., Li, Y., Dong, P. "Application of smoothed particle hydrodynamics for modeling the wave-moored floating breakwater interaction", Applied Ocean Research, 67, pp. 277–290, 2017.
https://doi.org/10.1016/j.apor.2017.07.011

[21] Domínguez, J. M., Crespo, A. J. C., Hall, M., Altomare, C., Wu, M., Stratigaki, V., Troch, P., Cappietti, L., Gómez-Gesteira, M. "SPH simulation of floating structures with moorings", Coastal Engineering, 153, 103560, 2019.
https://doi.org/10.1016/j.coastaleng.2019.103560

[22] Lyu, H.-G., Sun, P.-N., Huang, X.-T., Zhong, S.-Y., Peng, Y.-X., Jiang, T., Ji, C.-N. "A Review of SPH Techniques for Hydrodynamic Simulations of Ocean Energy Devices", Energies, 15(2), 502, 2022.
https://doi.org/10.3390/en15020502

[23] Domínguez, J. M., Fourtakas, G., Altomare, C., Canelas, R. B., Tafuni, A., …, Gómez-Gesteira, M. "DualSPHysics: from fluid dynamics to multiphysics problems", Computational Particle Mechanics, 9(5), pp. 867–895, 2022.
https://doi.org/10.1007/s40571-021-00404-2

[24] Amicarelli, A., Manenti, S., Albano, R., Agate, G., Paggi, M., …, Pirovano, G. "SPHERA v.9.0.0: A Computational Fluid Dynamics research code, based on the Smoothed Particle Hydrodynamics mesh-less method", Computer Physics Communications, 250, 107157, 2020.
https://doi.org/10.1016/j.cpc.2020.107157

[25] Abul-Azm, A. G., Gesraha, M. R. "Approximation to the hydrodynamics of floating pontoons under oblique waves", Ocean Engineering, 27(4), pp. 365–384, 2000.
https://doi.org/10.1016/S0029-8018(98)00057-2

[26] Sturova, I. V. "Effect of bottom topography on the unsteady behaviour of an elastic plate floating on shallow water", Journal of Applied Mathematics and Mechanics, 72(4), pp. 417–426, 2008.
https://doi.org/10.1016/j.jappmathmech.2008.08.012

[27] Meylan, M. H., Sturova, I. V. "Time-dependent motion of a two-dimensional floating elastic plate", Journal of Fluids and Structures, 25(3), pp. 445–460, 2009.
https://doi.org/10.1016/j.jfluidstructs.2009.01.001

[28] Sinha, A., Karmakar, D., Guedes Soares, C. "Shallow water effects on wave energy converters with hydraulic power take-off system", The International Journal of Ocean and Climate Systems, 7(3), pp. 108–117, 2016.
https://doi.org/10.1177/1759313116649966

[29] Havasi-Tóth, B. "Nauticle: A general-purpose particle-based simulation tool", Computer Physics Communications, 246, 106855, 2020.
https://doi.org/10.1016/j.cpc.2019.07.018

[30] Hafez, M. "Hydraulic analogy and visualisation of two-dimensional compressible fluid flows: part 1: theoretical aspects", International Journal of Aerodynamics, 6(1), pp. 41–66, 2018.
https://doi.org/10.1504/IJAD.2018.089765

[31] Wendland, H. "Piecewise polynomial, positive definite and compactly supported radial functions of minimal degree", Advances in Computational Mathematics, 4(1), pp. 389–396, 1995.
https://doi.org/10.1007/BF02123482

[32] Morris, J. P., Fox, P. J., Zhu, Y. "Modeling Low Reynolds Number Incompressible Flows Using SPH", Journal of Computational Physics, 136(1), pp. 214–226, 1997.
https://doi.org/10.1006/jcph.1997.5776

[33] Havasi-Tóth, B. "Reconstruction of 3D floating body motion on shallow water flows", In: Proceedings of the 17th SPHERIC International Workshop, Rhodes, Greece, 2023, pp. 294–301. ISBN 9781399958851

[34] Çelik, D., Khosravi, N., Khan, M. A., Waseem, M., Ahmed, H. "Advancements in nonlinear PID controllers: A comprehensive review", Computers and Electrical Engineering, 129, 110775, 2026.
https://doi.org/10.1016/j.compeleceng.2025.110775

[35] Williams, G. S., Hazen, A. "Hydraulic Tables: The Elements of Gagings and the Friction of Water Flowing in Pipes, Aqueducts, Sewers, Etc.", John Wiley & Sons, London, UK, 1910. [online] Available at: http://www.survivorlibrary.com/library/hydraulic_tables_of_gagings_and_friction_of_water_flowing_in_pipes_1909.pdf [Accessed: 11 November 2025]

[36] Schmitt, P., Windt, C., Davidson, J., Ringwood, J. V., Whittaker, T. "Beyond VoF: alternative OpenFOAM solvers for numerical wave tanks", Journal of Ocean Engineering and Marine Energy, 6(3), pp. 277–292, 2020.
https://doi.org/10.1007/s40722-020-00173-9

[37] ANSYS, Inc. "ANSYS AQWA, (2024 R1)", [computer program] Available at: https://www.ansys.com/products/structures/ansys-mechanical [Accessed: 11 November 2025]

[38] Gourlay, T., von Graefe, A., Shigunov, V., Lataire, E. "Comparison of *AQWA*, *GL Rankine*, *MOSES*, *OCTOPUS*, *PDStrip* and *WAMIT* With Model Test Results for Cargo Ship Wave-Induced Motions in Shallow Water", In: Proceedings of the ASME 2015 34th International Conference on Ocean, Offshore and Arctic Engineering, St. John's, Newfoundland, Canada, 2015, V011T12A006. ISBN 978-0-7918-5659-8
https://doi.org/10.1115/OMAE2015-41691